Intrinsic Functional Connectivity of Dentate Nuclei in Autism Spectrum Disorder

Sheeba Arnold Anteraper,[1–3,*] Xavier Guell,[3,4,*] Hoyt Patrick Taylor,[5] Anila D'Mello,[3]
Susan Whitfield-Gabrieli,[2,3] and Gagan Joshi[1,6]

Abstract

Cerebellar abnormalities are commonly reported in autism spectrum disorder (ASD). Dentate nuclei (DNs) are key structures in the anatomical circuits linking the cerebellum to the extracerebellum. Previous resting-state functional connectivity (RsFc) analyses reported DN abnormalities in high-functioning ASD (HF-ASD). This study examined the RsFc of the DN in young adults with HF-ASD compared with healthy controls (HCs) with the aim to expand upon previous findings of DNs in a dataset using advanced, imaging acquisition methods that optimize spatiotemporal resolution and statistical power. Additional seed-to-voxel analyses were carried out using motor and nonmotor DN coordinates reported in previous studies as seeds. We report abnormal dentato-cerebral and dentato-cerebellar functional connectivity in ASD. Our results expand and, in part, replicate previous descriptions of DN RsFc abnormalities in this disorder and reveal correlations between DN-cerebral RsFc and ASD symptom severity.

Keywords: autism spectrum disorder; cerebellum; dentate nucleus; functional connectivity; resting state networks; social cognition

Introduction

AUTISM SPECTRUM DISORDER (ASD) is a neurodevelopmental disorder characterized by deficits in social–emotional functioning along with restricted repetitive behaviors (APA, 2013). Although the associated psychopathologies as well as the combination and severity of symptoms are heterogeneous in ASD populations, cerebellar abnormalities are consistently observed in neuroimaging research in ASD (D'Mello and Stoodley, 2015). Observed cerebellar/cerebro-cerebellar circuit abnormalities in ASD include reduced integrity of white matter (WM) tracts linking the cerebellum to extracerebellar structures (Brito et al., 2009; Groen et al., 2011; Hanaie et al., 2013; Jeong et al., 2012; Shukla et al., 2010), abnormal gray matter volume in the cerebellar cortex (D'Mello et al., 2015; Rojas et al., 2006), disrupted resting-state functional connectivity (RsFc) between regions within the cerebellum and from the cerebellum to cerebrum (Arnold Anteraper et al., 2018; Khan et al., 2015; Noonan et al., 2009), and disruptions in lateralization of both function and structure of cerebellar and cerebral cortical regions (Dawson et al., 1982; Escalante-Mead et al., 2003).

The dentate nuclei (DNs), the largest of the four pairs of cerebellar nuclei, are highly convoluted clusters of neurons embedded in the WM of the cerebellum (Sultan et al., 2010). The DNs play a role in cognitive, affective, and motor domains of behavior and are part of anatomical circuits linking the cerebellar cortex, thalamus, cerebral cortex, and basal ganglia (Alahmadi et al., 2017; Bernard et al., 2014; Bostan et al., 2010; Dum and Strick, 2003; Habas, 2010; Hoshi et al., 2005; Kuper et al., 2011). Tract-tracing studies demonstrate DN anatomical connectivity to motor cortical areas (BA 4,6) and nonmotor cognitive areas such as medial, dorsolateral, and orbital prefrontal cortices (Dum and Strick, 2003). The cerebellum's extended developmental

---

[1]Alan and Lorraine Bressler Clinical and Research Program for Autism Spectrum Disorder, Massachusetts General Hospital, Boston, Massachusetts.
[2]Department of Psychology, Northeastern University, Boston, Massachusetts.
[3]Department of Brain and Cognitive Sciences, Massachusetts Institute of Technology, Cambridge, Massachusetts.
[4]Department of Neurology, Massachusetts General Hospital and Harvard Medical School, Boston, Massachusetts.
[5]Department of Physics, University of North Carolina, Chapel Hill, North Carolina.
[6]Department of Psychiatry, Harvard Medical School, Boston, Massachusetts.
*These two authors contributed equally to this article.

trajectory makes it susceptible to dysfunction arising from genetic and epigenetic factors leading to potential deficits in neuroplasticity, sensorimotor processing, and multisensory integration (Sathyanesan et al., 2019). Synaptic and morphological defects of Purkinje cells (PCs) are potentially a key feature of developmental disorders with cerebellar dysfunction. A decrease in the number of PCs in autism, especially in Crus II in the posterior inferior hemisphere, which project to the dentate, has been reported before (Skefos et al., 2014). Previous studies have also reported dysregulation of GABA activity and decreased parvalbumin in PCs in cerebellar Crus II (Soghomonian et al., 2017; Yip et al., 2007).

The cerebellum is involved in regulation and modulation of affective and cognitive processes, in addition to motor processes (Guell et al., 2018b; Kelly and Strick, 2003; Middleton and Strick, 1994; Schmahmann and Sherman, 1998; Schmahmann, 1996; Stoodley and Schmahmann, 2009; Stoodley et al., 2012). There are several hypotheses regarding the specific role of the cerebellum in nonmotor and motor processes, including error-driven learning, prediction, timing of events, sequencing, and generation of internal models (Guell et al., 2018a). Importantly, the dorsal and ventral aspects of the DN are functionally distinct. The dorsal DN contributes to motor processes, while the ventral DN contributes to nonmotor processes (Alahmadi et al., 2017; Bernard et al., 2014; Dum and Strick, 2003). Diffusion tensor imaging studies have confirmed this functional topography of the DN, with connectivity between the dorsal DN and motor aspects of the cerebellum (lobules IV, V, and VI) and between the ventral DN and nonmotor aspects of the cerebellum (Crus I/II) (Steele et al., 2017).

Within the framework of control theory, which uses dynamical systems modeling to predict and design the response of systems to input, the brain has an internal model of the world that predicts what inputs it should be receiving. The cerebellum receives inputs from motor and nonmotor regions of the brain and has the machinery to attempt to reduce prediction error between this model and the incoming physiological signals by either updating the model or by taking action (Ramnani, 2014). In light of the histological homogeneity, it has been postulated that the cerebellum may play an analogous role in both motor and nonmotor functions regulating the speed, appropriateness, and timing of motor, cognitive, and affective processes (Schmahmann and Sherman, 1998). In contrast to the cerebral cortex where variation in cytoarchitecture largely coincides with variation in function (Brodmann, 2006), the functional variations across the cerebellar cortex are defined by its anatomical connections to extracerebellar structures (Ito, 1993; Schmahmann, 1991) and manifest as functional territories (FTs), as revealed by task-based and functional connectivity studies (Diedrichsen et al., 2019). Motor regions of the cerebellum form reciprocal circuits with somatomotor regions of the cerebral cortex, while nonmotor regions of the cerebellum interact with cognitive and affective regions of the cerebral cortex (Kelly and Strick, 2003). Previous work using a combination of functional magnetic resonance imaging (fMRI), positron emission tomography (PET), viral tracing, and animal models has characterized the circuitry underlying these interactions: information from each cerebral cortical hemisphere is directed to the ipsilateral pons; information from the pons is directed to the contralateral cerebellar cortex through

the middle cerebellar peduncles; PC efferents in the cerebellar cortex project to the ipsilateral DNs; and information leaves the DN through the superior peduncles to the contralateral thalamus, which relays information back to the original region of the cerebral cortex (Buckner, 2013).

A large number of studies have reported cerebellar-cortical functional connectivity differences in ASD (e.g., Arnold Anteraper et al., 2018), but very few have focused on cerebellar nucleus abnormalities. Olivito and colleagues (2017) reported abnormal functional connectivity between the DN and cerebral cortical regions involved in the theory of mind processing. Hanaie and colleagues (2018) performed whole-brain, seed-based RsFc analyses using the bilateral DN and subregions of the cerebellar cortex (20 lobules and 8 vermis regions) as regions of interest in two independent datasets, and they reported reduced right DN to cerebral cortex connectivity in the ASD group. Based on the possibility that cerebellar nuclei and cerebral cortical contributions to neural function are fundamentally distinct (Raymond and Medina, 2018), it is relevant to further investigate DN functional connectivity differences in ASD. In this study, we aim to expand upon previous findings of DNs in a dataset using advanced imaging acquisition methods that optimize spatio-temporal resolution and statistical power. A male-only sample was chosen in line with recent reports suggesting that cortico-cerebellar functional connectivity patterns might be distinct in males, as opposed to female ASD patients (Smith et al., 2019).

Methods

Study participants

Our study and analysis included 20 ASD participants and 20 healthy controls (HCs) (all males), mean ages = 21.25 ± 3.73 and 24.15 ± 3.88 years, respectively (see Table 1 for demographics). MRI and behavioral data were obtained from the Autism Brain Imaging Data Exchange (ABIDE) dataset provided by Michal Assaf, MD (Olin Neuropsychiatry Research Center, Institute of Living, Hartford Hospital and Yale School of Medicine, Department of Psychiatry) (Di Martino et al., 2014). Detailed information on phenotypic assessments and scan procedures is available at http://fcon_1000.projects.nitrc.org/indi/abide/abide_II.html To be included as participants with ASD, individuals met a diagnostic cutoff score for ASD at the Autism Diagnostic Observation Schedule–Generic (ADOS-G) (Lord et al., 2000). Enrollment as an HC required ruling out any psychiatric disorder based on the Structured Clinical Interview for DSM-IV Axis I Disorders-Research Version (First et al., 1996) and the ADOS-G.

Data acquisition

MRI resting-state and structural data provided by the ABIDE dataset were acquired as follows. Resting-state echo-planar images (EPI) were collected on 3T Siemens Skyra with simultaneous multislice imaging (multiband factor = 8), repetition time (TR) = 475 msec, echo time (TE) = 30 msec, flip angle (FA) = 60°, and with 3-mm isotropic voxels, 947 volumes with whole-brain coverage. T1-weighted structural images were collected using TR/TE/inversion time/FA: 2200 msec/2.88 msec/794 msec/13° and 0.8-mm isotropic voxels.

	ASD	HC	p-Value
Demographics			
Total participants	20 (all male)	20 (all male)	
Age (years)			
Mean (range)	21.25 ± 3.73 (18–31)	24.15 ± 3.88 (19–30)	$p = 0.021$
<18 years	0 (0)	0 (0)	
Right-handedness	18 (90)	20 (100)	
Full-scale IQ (range)	112.05 ± 12.33 (80–146)	113 ± 11.06 (85–146)	n.s
Total ADOS-G	9.52 ± 2.04 (6–14)	1.95 ± 1.43 (0–5)	$p < 0.001$
Quality control metrics			
Mean head motion	0.12	0.12	n.s
Max head motion	1.8	1.37	n.s
Average global BOLD signal changes observed (after denoising)	0.81	0.77	n.s

Values are expressed as n (%) or mean ± standard deviation.

ASD, autism spectrum disorder; BOLD, blood-oxygen-level-dependent; HCs, healthy controls; IQ, intelligence quotient; ADOS-G, Autism Diagnostic Observation Schedule–Generic; n.s., not significant.

Seed selection

Seed-based RsFc analysis was carried out using left and right dentate seeds shown in Figure 1A (2-mm isotropic dentate atlas in the Montreal Neurological Institute (MNI) space provided by https://can.ucr.edu/software) derived from quantitative susceptibility mapping (QSM) (He et al., 2017). Compared with seeds drawn from T2-weighted or susceptibility-weighted images, the QSM-based method for seed selection is better suited for extracting time courses from the DN, a structure that is buried in WM, as it provides better delineation of boundaries. In addition, this method yields comparatively better probability of overlap with individual segmentation (He et al., 2017). Additional analyses were added using motor and nonmotor FTs centered around the dorsal dentate (−12, −57, −30) and ventral dentate (−17, −65, −35), respectively (Fig. 1B), based on the study by Bernard and associates (2014) (2-mm radius spheres).

Data analysis

Before carrying out the RsFc analysis, EPI data were preprocessed in SPM12 (realignment with respect to the first volume, normalization to MNI space with respect to the EPI template, and spatial smoothing with a 6-mm kernel [4-mm kernel for motor and nonmotor FTs]) (Wellcome Department of Imaging Neuroscience, London, United Kingdom; http://fil.ion.ucl.ac.uk/spm). Additional preprocessing steps were carried out using the CONN toolbox (Whitfield-

Gabrieli and Nieto-Castanon, 2012). This included band pass filtering (0.008–0.1 Hz), physiological signal denoising to eliminate contributions from WM and cerebrospinal fluid (using the anatomical component-based noise correction method (Behzadi et al., 2007), and regressing out movement effects and their first-order derivatives along with motion outliers (identified with artifact detection tools [ART] [http://nitrc.org/projects/artifact_detect], scan-to-scan threshold <0.5 mm, and global mean signal <3 standard deviations of mean). Of note, the time series data that were used to extract the blood-oxygen-level-dependent (BOLD) signal from the dentate seeds for seed-to-voxel analyses were unsmoothed. For first-level, seed-based RsFc analysis, Pearson's correlation coefficients were generated by computing correlations between the seed time series and time series of the rest of the voxels in the brain volume. These seed-to-voxel r maps were then transformed to z maps using Fisher's r-to-z transformation and brought up to a general linear model analysis at the second level for within-group and between-group comparisons. There were no significant differences in mean or maximum head motion between groups. However, age was significantly higher ($p = 0.021$) in the HC group and was therefore included as a regressor of no interest for between-group comparisons.

Within- and between-group results were thresholded using a whole-brain height threshold of $p < 0.001$ and false discovery rate (FDR)-corrected cluster threshold of $p < 0.05$. To further interpret the functional significance of our results, cerebellar clusters were plotted in a gradient space of
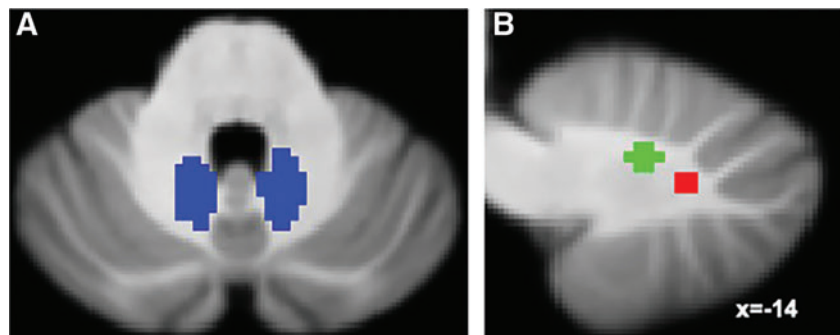

FIG. 1. (A) Quantitative susceptibility mapping-based seed location (He et al., 2017) for left and right DNs. (B) Motor (green) and nonmotor (red) seed locations based on the study by Bernard and colleagues (2014). DN, dentate nucleus. Color images are available online.

cerebellar functional neuroanatomy derived from 1003 Human Connectome Project participants [see Guell et al. (2018c)] using our in-house developed software, LittleBrain (Guell et al., 2019b). The SUIT toolbox was used to visualize cerebellar results using cerebellar flat maps (Diedrichsen and Zotow, 2015). For the additional exploratory analysis of unique effect [comparison of nonmotor vs. motor DN seeds, Bernard et al. (2014)], within- and between-group results were thresholded using a whole-brain height threshold of $p < 0.005$ and FDR-corrected cluster threshold of $p < 0.05$.

Results

Between-group contrast of DN functional connectivity

From the right DN seed, functional connectivity in the ASD group compared with HCs was reduced with ipsilateral supramarginal gyrus (SMG) and contralateral cerebellar lobules VI, Crus I, Crus II, VIIB, and VIII (Fig. 2A, B).

There were no statistically significant between-group differences in functional connectivity from the left DN seed.

Inspection of within-group maps of connectivity from right DNs in the HC group (Fig. 2E) and ASD group (Fig. 2F) revealed, as expected from between-group findings shown in Figure 2A and B, stronger connectivity in the HC group in the ipsilateral cerebral cortex and contralateral cerebellum when compared with the ASD within-group DN connectivity maps (including absent positive functional connectivity, as determined by our thresholds, to the right SMG and some aspects of left cerebellar cortex in ASD). There was increased connectivity to the posterior cingulate cortex and medial prefrontal cortex in ASD maps when compared with HC maps (Fig. 2E, F), but these differences that were observable in within-group maps did not survive statistical testing in our group contrast analysis (Fig. 2A, B). Detailed cluster information for between-group results is presented in Table 2 as well as Figure 2G.
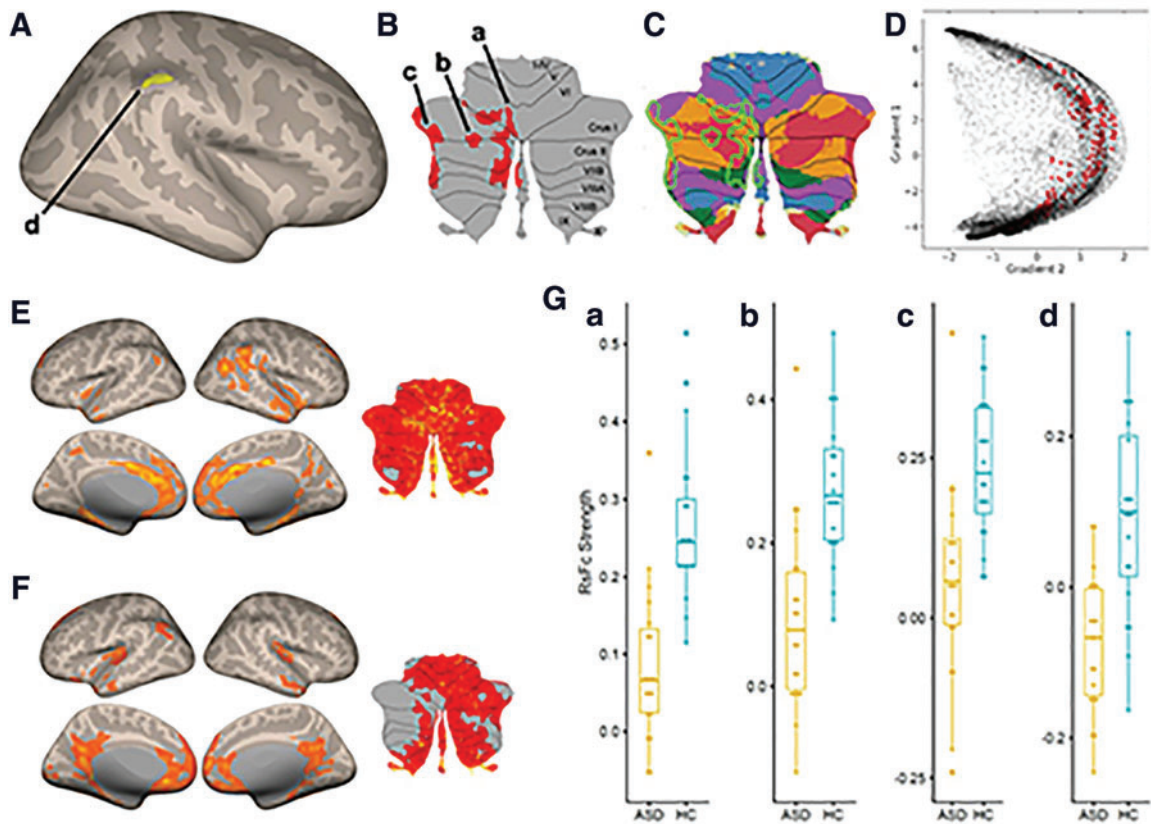

FIG. 2. **(A)** Cerebral cortical results from between-group seed-to-voxel RsFc analysis for HC > ASD contrast (two-sided) for right DN at a height threshold of whole brain, $p < 0.001$ (T = 3.57), and FDR-corrected cluster threshold of $p < 0.05$. Age was added as a regressor of no interest. **(B)** Cerebellar results of the same contrast presented in a cerebellar flat map (Diedrichsen and Zotow, 2015). Cluster labels in **(A)** and **(B)** correspond to Table 2. **(C)** Cerebellar cluster shown in **(B)** overlaid on cerebellar representations of cerebral cortical networks (Buckner et al., 2011): dark purple, visual; blue, somatomotor; green, dorsal attention; violet, ventral attention; cream, limbic; orange, frontoparietal; and red, default network. **(D)** Cerebellar cluster shown in **(B)** represented in the functional gradient space as developed by Guell and colleagues (2018c). Each dot represents one cerebellar voxel; dots shown in color correspond to the voxels that are included in the cerebellar cluster shown in **(B)**. **(E)** HC within-group connectivity from the right DN seed at a height threshold of whole brain, $p < 0.001$, and FDR-corrected cluster threshold of $p < 0.05$. **(F)** ASD within-group connectivity from the right DN seed using the same thresholds as in **(E)**. **(G)** Boxplots of ASD and HC connectivity data extracted from clusters shown in **(A)** and **(B)**. HCs, healthy controls; ASD, autism spectrum disorder; FDR, false discovery rate; RsFc, resting-state functional connectivity. Color images are available online.

TABLE 2. RESULTS FROM SECOND-LEVEL SEED-TO-VOXEL RSFC ANALYSIS FOR HC VERSUS ASD CONTRAST
FOR RIGHT DN (HEIGHT THRESHOLD = $P < 0.001$ TWO-SIDED; CLUSTER THRESHOLD = $P < 0.05$ FDR CORRECTED)

Cluster label	Brain region of each cluster	Peak cluster coordinates (MNI)	Voxels per cluster	T_{max}
a	Cerebellum (lobules VI, Crus I, Crus II, VIIB), left	$-06 - 72 - 38$	159	6.10
b	Cerebellum (Crus I, Crus II), left	$-24 - 66 - 36$	122	5.24
c	Cerebellum (Crus I, Crus II, VIIB), left	$-32 - 44 - 40$	109	5.37
d	Supramarginal gyrus, right	$48 - 36 \ 44$	105	4.65

FDR, false discovery rate; RsFc, resting-state functional connectivity; DN, dentate nucleus; MNI, Montreal Neurological Institute.

Inspection of within-group functional connectivity maps from the additional seed-to-voxel analysis of unique effect (nonmotor > motor DN seeds) in HCs (Fig. 3A) and ASD (Fig. 3B) revealed stronger connectivity in right Crus I/II in the HC group. Direct comparison (HC vs. ASD contrast) revealed increased connectivity to posterior cingulate and superior frontal cortices, associative visual cortex, fusiform gyri, and superior temporal regions (Fig. 4). Detailed cluster information for between-group results is presented in Table 3.

Within-group ASD behavioral correlations with DN functional connectivity

Within-group ASD behavioral correlations with total ADOS scores were carried out on all the clusters that sur-

vived significance testing for the between-group contrasts. Results are shown in Figure 5.

Discussion

In the present study, we examined whole-brain RsFc of the DN in ASD using high spatial and temporal fMRI resolution as well as QSM-based DN seeds. Our findings provide evidence of abnormal intrinsic functional connectivity of the DN in young adults with high-functioning ASD (HF-ASD). Specifically, we report decreased connectivity with SMG and multiple cerebellar cortical territories. Our findings are consistent with a large body of evidence demonstrating cerebellar functional connectivity abnormalities in ASD (Arnold Anteraper et al., 2018; Khan et al., 2015; Verly et al., 2014)
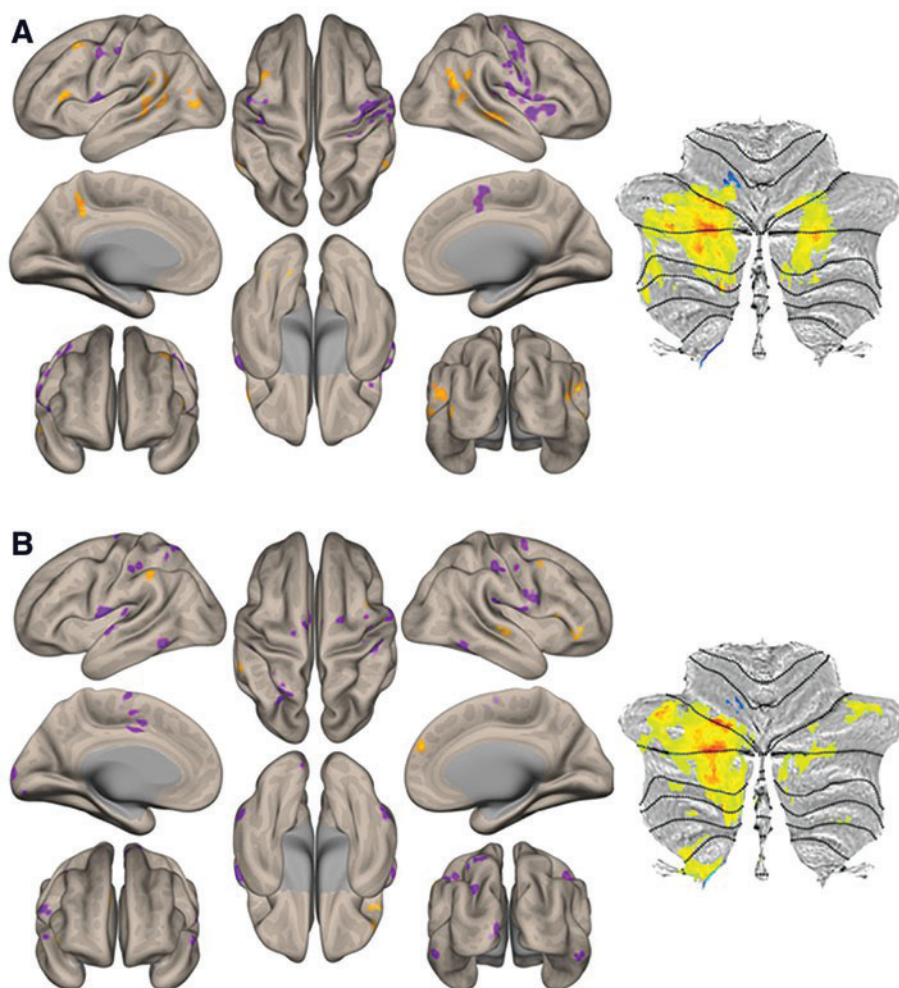

FIG. 3. HC (A) and ASD (B) within-group connectivity for the unique effect (nonmotor > motor DN seeds) at a height threshold of whole brain, $p < 0.005$, and FDR-corrected cluster threshold of $p < 0.05$. Cerebellar results are presented on a flat map (Diedrichsen and Zotow, 2015). Color images are available online.
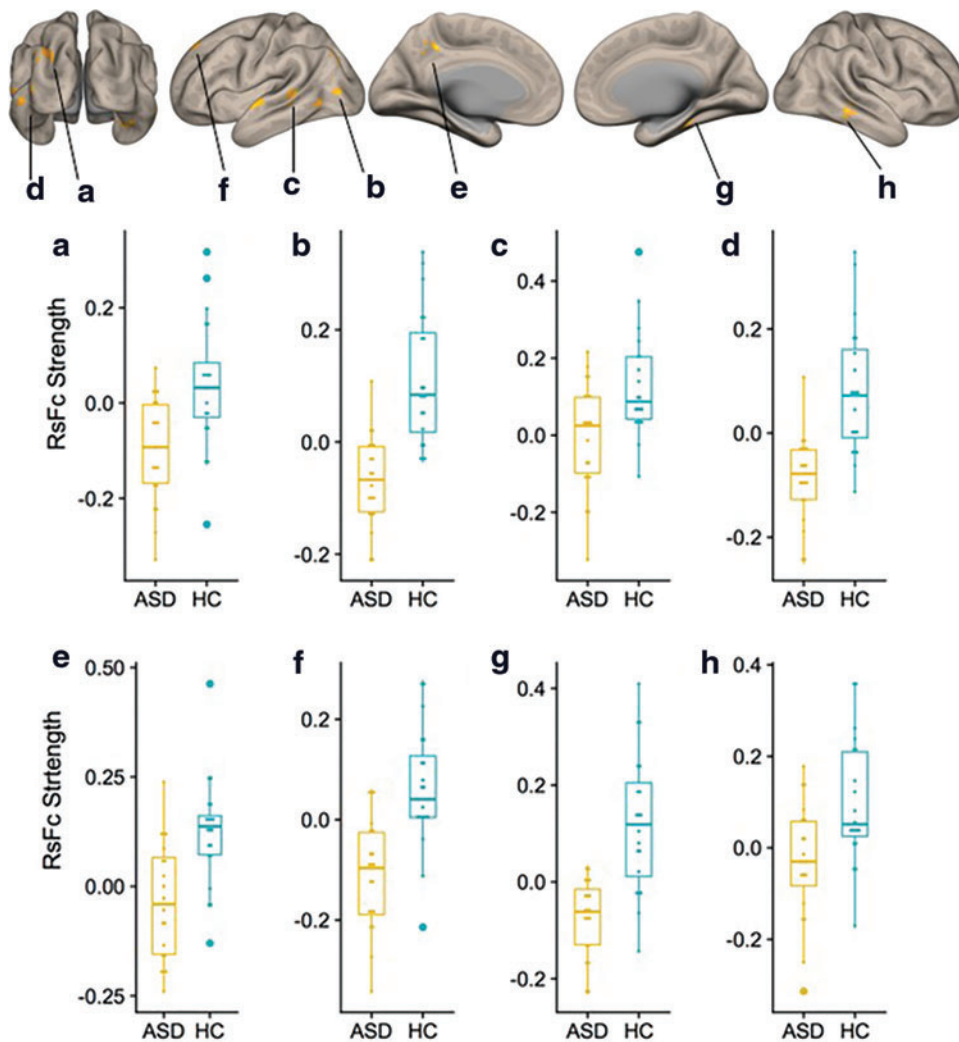
FIG. 4. Cerebral cortical results from second-level seed-to-voxel RsFc analysis for HC versus ASD contrast for the unique effect (nonmotor > motor DN seeds) (height threshold = $p < 0.005$; cluster threshold = $p < 0.05$ FDR corrected). Age was added as a regressor of no interest. Boxplots **(a–h)** correspond to RsFc strength extracted from clusters a through h (cluster labels correspond to Table 3). Color images are available online.

and extend previous findings of abnormal functional connectivity of the DN in this disorder (Olivito et al., 2017) in a more stringent statistical analysis using a dataset with higher spatial and temporal resolution and a refined seed selection method.

Recent studies indicate that cerebellar nuclei might play a relevant and functionally distinct role in the anatomical circuits linking the cerebellar cortex with extracerebellar regions (Raymond and Medina, 2018). If the DN performs a distinct computation when compared with the cerebellar cortex, a comprehensive analysis of cerebellar functional connectivity in ASD should include the DN. This hypothesis, in combination with previous evidence of abnormal RsFc of the DN in ASD (Olivito et al., 2017), highlights the

TABLE 3. RESULTS FROM SECOND-LEVEL SEED-TO-VOXEL RsFc ANALYSIS FOR HC VERSUS ASD CONTRAST FOR THE UNIQUE EFFECT (NONMOTOR > MOTOR DN SEEDS) (HEIGHT THRESHOLD = $P < 0.005$; CLUSTER THRESHOLD = $P < 0.05$ FDR CORRECTED)

Cluster label	Brain region of each cluster	Peak cluster coordinates (MNI)	Voxels per cluster	T_{max}
a	Left visual association area	$-26 - 62 + 24$	260	5.21
b	Left fusiform gyrus (FG)	$-54 - 66 - 04$	136	6.58
c	Left superior temporal sulcus (STS)	$-54 - 40 + 06$	116	4.79
d	Left superior temporal gyrus	$-58 - 06 - 04$	109	5.96
e*	Precuneous/posterior cingulate cortex	$-06 - 44 + 42$	96	4.69
f*	Frontal pole/superior frontal gyrus	$-14 + 44 + 48$	94	4.91
g	Right FG	$+38 - 28 - 24$	91	5.30
h	Right STS	$+58 - 38 - 10$	83	5.58

*Denotes regions (clusters e and f) that are significantly correlated with total ADOS scores, see Figure 5.
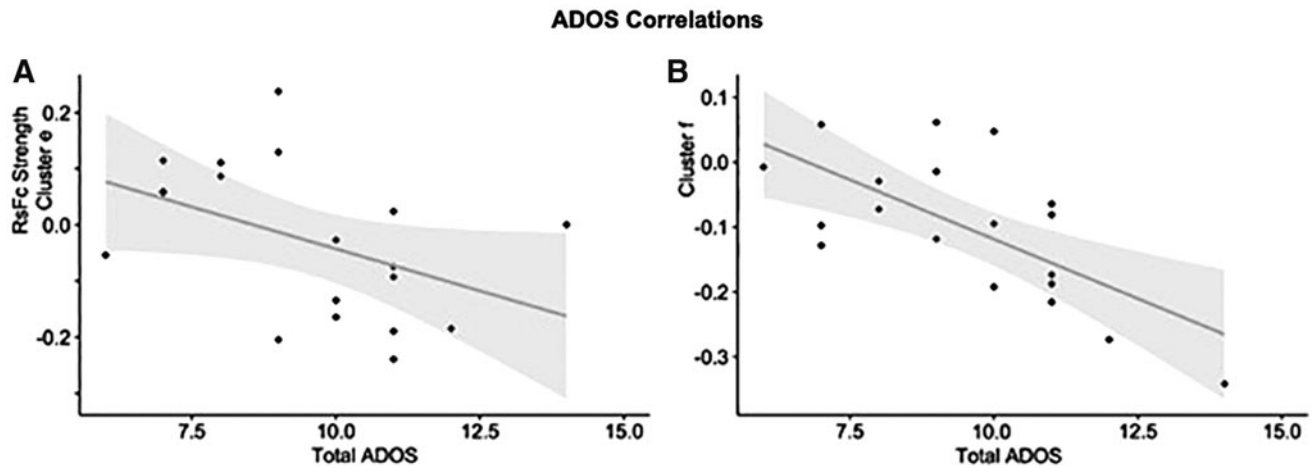
ADOS Correlations

FIG. 5. Group differences in dentate connectivity for the unique effect (nonmotor > motor DN) correlate with total Autism Diagnostic Observation Schedule scores in the posterior cingulate cortex (**A**) and superior frontal gyrus (**B**).

relevance of investigating the functional connectivity of DN in ASD.

Abnormal dentato-cerebral connectivity in ASD

Cerebral-cortical functional connectivity abnormalities were observed in a task-positive region, specifically in the right SMG (Fig. 2A). Cerebellar-cortical functional connectivity abnormalities were situated in both task-negative (default mode) and task-positive (frontoparietal, ventral attention, and dorsal attention network) regions. The DN receives input from many different aspects of the cerebellar cortex, clinical phenomenology in ASD includes disruption of numerous aspects of cognitive and affective processing, and it is thus reasonable to observe abnormal connectivity in both task-negative and task-positive regions in our analysis. DN connectivity abnormalities to SMG have been reported in previous investigations of DN functional connecitivty in ASD (Olivito et al., 2017). Previous RsFc studies have shown that the DN has strong functional coherence with SMG (Allen et al., 2005). SMG has been implied in human action observation/imitation and is noted to be functionally abnormal in fMRI investigations in ASD (Salmi et al., 2013). Functional hypoconnectivity in dorsal and ventral attention networks in adults with ASD has also been reported before (Farrant and Uddin, 2016). Subregions of the temporoparietal junction (TPJ), such as the SMG, are part of the somatosensory association cortex, have functional associations with cerebellar cortices (specifically with left Crus II of the cerebellum) (Igelstrom et al., 2017), and are also implicated in identification of gestures and postures of others as a part of the mirror neuron system (Reed and Caselli, 1994) that is affected in ASD. Furthermore, one transcranial magnetic stimulation study (Riva et al., 2016) determined causal involvement of the right SMG in emotional egocentricity biasing (Silani et al., 2008). The right TPJ is also consistently implicated in false belief tasks wherein subjects are asked to predict the behavior of someone who has received invalid information (Saxe and Wexler, 2005). Children with ASD show delayed development in performance on such tasks versus age-matched controls (Baron-Cohen, 1989).

Lack of anticorrelations between the default mode network (DMN) and right SMG has been demonstrated recently in two different adult cohorts of HF-ASD (Joshi et al., 2017). While our present analysis did not investigate connectivity between the DMN and right SMG, our between-group DN connectivity contrast revealed abnormalities in both the cerebellar DMN and right SMG. Abnormal connectivity of the DMN and SMG with DN resonates with our previous description of dysconnectivity between these two networks in ASD (Joshi et al., 2017). In this way, our results are coherent with previous studies, suggesting that disruptions in task-positive/task-negative interactions are a core feature of ASD (Joshi et al., 2017; Kennedy and Courchesne, 2008; Yerys et al., 2015).

Abnormal dentato-cerebellar connectivity in ASD

The right DN was abnormally connected with numerous distinct FTs of the cerebellum in the ASD group. Left cerebellar functional abnormalities, specifically in each of the three areas of cerebellar nonmotor representation, have been reported recently using a high-temporal resolution, unbiased, data-driven fMRI analysis (Arnold Anteraper et al., 2018).

Cerebellar regions of abnormal RsFc with the right DN spanned through multiple distinct FTs of the cerebellar cortex, including ventral attention, dorsal attention, frontoparietal, and DMNs, as well as some aspects of the somatomotor network (Fig. 2C). Visualizing our results in a cerebellar functional gradient space as developed by Guell and colleagues (2018c) confirmed that our results were not restricted to one single functional domain of the cerebellum, but rather spanned across multiple territories in a continuous motor-to-nonmotor distribution (as indicated by the wide spread of data points along gradients 1 and 2 in Fig. 2D). This organization is coherent with the anatomical reality that the DN receives input from many different aspects of the cerebellar cortex and is consistent with the wide diversity of behavioral abnormalities observed in ASD (ranging from sensory to motor to multiple domains of cognitive and affective processing).

Abnormal connectivity in right, but not left, DN

Our analysis revealed abnormal functional connectivity in right, but not left, DN. This observation is in contrast to a previous study reporting left, but not right, DN functional dysconnectivity in ASD (Olivito et al., 2017). However, a voxel-based morphometry analysis by the same research group revealed structural differences in the regional cerebellar gray matter volume (GMV), specifically in right Crus II (Olivito et al., 2018). More recently, Hanaie and colleagues (2018) have reported reduced RsFc of the right DN in ASD. While additional studies with larger cohorts will be needed to definitively characterize the predominance of left versus right DN abnormal connectivity in ASD, convergent evidence from animal and human ASD research indicates that the right cerebellum (and thus right DN) might play a more important role in the pathophysiology of ASD when compared with the left cerebellum. Specifically, previous studies in children with ASD report reduced cerebellar GMV in the right cerebellum (D'Mello et al., 2015). Reductions in right cerebellar GMV have been associated with core ASD symptomology (D'Mello et al., 2015). The importance of the right cerebellum compared with the left has also been explored in animal studies of ASD. Stoodley and colleagues (2017) reported that neuromodulation of the right, but not left, cerebellum was sufficient to both cause and rescue social communication deficits in a mouse model of ASD. Although it is not clear why this lateralization exists, it may be the case that the right cerebellum is more specialized for socio-communicative functions through its contralateral connectivity with left cerebral regions implicated in language. Deficits in socio-communicative skills are core to the ASD diagnosis.

Of note, no significant differences were observed when directly comparing seed-to-voxel functional connectivity between the two hemispheres. In this way, while our analyses revealed differences in the right, but not left, DN, future studies with higher statistical power will be needed to definitively establish lateralization differences in DN abnormalities in ASD.

Unique effect (nonmotor vs. motor DNs)

Additional analyses exploring the unique effect [comparison of nonmotor vs. motor DN seeds, Bernard et al. (2014)] revealed significant differences in both task-positive and task-negative networks. ASD participants showed decreased strengths in functional connectivity in the posterior cingulate and superior frontal cortices (Fig. 4, clusters e and f), both nodes of the DMN. DMN is one of the most consistently abnormal networks in ASD studies [for review, see Padmanabhan et al. (2017)]. Our findings of DN-DMN connectivity abnormalities provide further support for a central role of DMN in ASD. DN connectivity abnormalities were also observed in task-positive regions, specifically in the associative visual cortex (Fig. 4, cluster a), fusiform gyri (clusters b and g), and superior temporal regions (clusters c, d, and h). These regions are associated with social processing, and poor functional segregation of these regions with DMN has been previously reported (Joshi et al., 2017). Hypoactivation in fusiform gyri to emotional face processing has been reported previously (Pelphrey, 2017). Connectivity between left Crus I/II and bilateral, posterior, superior temporal regions is associated with social interaction (Jack and Pelphrey, 2015), which is one of the core deficits of ASD. Very recent reports suggest that network-based (as opposed to location-based) characterization of fMRI abnormalities might crucially improve the consistency of findings across neuroimaging studies of specific neurological and psychiatric disorders (Darby et al., 2018). DN receives input from many different aspects of the cerebellar cortex, clinical phenomenology in ASD includes disruption of numerous aspects of cognitive and affective processing, and it is thus reasonable to observe abnormal connectivity in both task-negative (DMN) and task-positive regions in our analysis.

Behavioral correlations

This is the first study to establish a correlation between ASD symptom severity and DN functional connectivity. Brain regions emerging from ADOS correlations, posterior cingulate cortex and superior frontal gyrus, align with clinically relevant features of ASD. These regions (part of the DMN) are relevant for internally oriented thought and conceiving the perspective of others, which are brain functions that are abnormal in ASD. Importantly, these brain regions that are abnormally connected to DNs in ASD are also the brain regions that are more strongly correlated with symptom severity when analyzing connectivity patterns to the DN. The correspondence of between-group differences and within-group ADOS correlations observed here provides further evidence that the structures identified in our analysis are relevant in the pathophysiology of ASD and hone in on the relevance of studying the DN in ASD.

Limitations and future studies

The findings of the present study invite future investigations to continue exploring the role of the DN in ASD. In this study, the entire DN (rather that subsections) was used as the seed for RsFc analysis. Future studies may be able to obtain a more nuanced understanding of the role of the DN in ASD by conducting RsFc analysis with smaller FTs within the DN (Guell et al., 2019a). However, given the resolution limitations of current fMRI methods, this may be difficult without higher field strengths or denser array coils. Behavioral correlations in studies with modest sample sizes are inherently limited (Button et al., 2013). Because of the clinical heterogeneity in autism, studies with larger sample sizes will be needed to definitively establish that DN functional connectivity abnormalities correlate with symptom severity in ASD. This limitation notwithstanding, our study is the first to identify a relationship between ASD symptom severity and DN functional connectivity and thus invites future larger investigations to continue exploring not only differences in DN connectivity between ASD patients and controls but also the relationship between DN fMRI signals and clinical severity within ASD cohorts. As the unique role of the DN in cerebellar processing is only beginning to be understood (Raymond and Medina, 2018), interesting questions about its contribution to ASD remain open. Future studies may examine whether DN abnormalities are different from cerebellar cortical abnormalities and whether abnormal DN physiology makes unique contributions to ASD phenotypes.

Acknowledgments

Author Disclosure Statement

Funding Information

References

Alahmadi AA, Pardini M, Samson RS, Friston KJ, Toosy AT, D'Angelo E, Gandini Wheeler-Kingshott CA. 2017. Cerebellar lobules and dentate nuclei mirror cortical force-related-BOLD responses: beyond all (linear) expectations. Hum Brain Mapp 38:2566–2579.

Allen G, McColl R, Barnard H, Ringe WK, Fleckenstein J, Cullum CM. 2005. Magnetic resonance imaging of cerebellar-prefrontal and cerebellar-parietal functional connectivity. Neuroimage 28:39–48.

APA. 2013. *Diagnostic and Statistical Manual of Mental Disorders,* 5th ed. Arlington, VA: American Psychiatric Association.

Arnold Anteraper S, Guell X, D'Mello A, Joshi N, Whitfield-Gabrieli S, Joshi G. 2018. Disrupted cerebrocerebellar intrinsic functional connectivity in young adults with high-functioning autism spectrum disorder: a data-driven, whole-brain, high-temporal resolution functional magnetic resonance imaging study. Brain Connect 9:48–59.

Baron-Cohen S. 1989. The autistic child's theory of mind: a case of specific developmental delay. J Child Psychol Psychiatry 30:285–297.

Behzadi Y, Restom K, Liau J, Liu TT. 2007. A component based noise correction method (CompCor) for BOLD and perfusion based fMRI. Neuroimage 37:90–101.

Bernard JA, Peltier SJ, Benson BL, Wiggins JL, Jaeggi SM, Buschkuehl M, et al. 2014. Dissociable functional networks of the human dentate nucleus. Cereb Cortex 24:2151–2159.

Bostan AC, Dum RP, Strick PL. 2010. The basal ganglia communicate with the cerebellum. Proc Natl Acad Sci U S A 107:8452–8456.

Brito AR, Vasconcelos MM, Domingues RC, Hygino da Cruz LC, Jr., Rodrigues Lde S, Gasparetto EL, Calcada CA. 2009. Diffusion tensor imaging findings in school-aged autistic children. J Neuroimaging 19:337–343.

Brodmann K, Gary LJ. 2006. *Brodmann's Localisation in the Cerebral Cortex: The Principles of Comparative Localisation in the Cerebral Cortex Based on Cytoarchitectonics.* New York, NY: Springer.

Buckner RL. 2013. The cerebellum and cognitive function: 25 years of insight from anatomy and neuroimaging. Neuron 80:807–815.

Buckner RL, Krienen FM, Castellanos A, Diaz JC, Yeo BT. 2011. The organization of the human cerebellum estimated by intrinsic functional connectivity. J Neurophysiol 106:2322–2345.

Button KS, Ioannidis JP, Mokrysz C, Nosek BA, Flint J, Robinson ES, Munafo MR. 2013. Power failure: why small sample size undermines the reliability of neuroscience. Nat Rev Neurosci 14:365–376.

D'Mello AM, Crocetti D, Mostofsky SH, Stoodley CJ. 2015. Cerebellar gray matter and lobular volumes correlate with core autism symptoms. Neuroimage Clin 7:631–639.

D'Mello AM, Stoodley CJ. 2015. Cerebro-cerebellar circuits in autism spectrum disorder. Front Neurosci 9:408.

Darby RR, Joutsa J, Fox MD. 2018. Network localization of heterogeneous neuroimaging findings. Brain 142:70–79.

Dawson G, Warrenburg S, Fuller P. 1982. Cerebral lateralization in individuals diagnosed as autistic in early childhood. Brain Lang 15:353–368.

Di Martino A, Yan CG, Li Q, Denio E, Castellanos FX, Alaerts K, et al. 2014. The autism brain imaging data exchange: towards a large-scale evaluation of the intrinsic brain architecture in autism. Mol Psychiatry 19:659–667.

Diedrichsen J, King M, Hernandez-Castillo C, Sereno M, Ivry RB. 2019. Universal transform or multiple functionality? Understanding the contribution of the human cerebellum across task domains. Neuron 102:918–928.

Diedrichsen J, Zotow E. 2015. Surface-based display of volume-averaged cerebellar imaging data. PLoS One 10:e0133402.

Dum RP, Strick PL. 2003. An unfolded map of the cerebellar dentate nucleus and its projections to the cerebral cortex. J Neurophysiol 89:634–639.

Escalante-Mead PR, Minshew NJ, Sweeney JA. 2003. Abnormal brain lateralization in high-functioning autism. J Autism Dev Disord 33:539–543.

Farrant K, Uddin LQ. 2016 Atypical developmental of dorsal and ventral attention networks in autism. Dev Sci 19:550–563.

First M, Gibbon M, Williams J, Spitzer R. 1996. Structured Clinical Interview for DSM-IV Disorders: SCID SCREEN Patient Questionnaire Computer Program. Washington, DC: American Psychiatric Press.

Groen WB, Buitelaar JK, van der Gaag RJ, Zwiers MP. 2011. Pervasive microstructural abnormalities in autism: a DTI study. J Psychiatry Neurosci 36:32–40.

Guell X, Gabrieli JDE, Schmahmann JD. 2018a. Embodied cognition and the cerebellum: perspectives from the dysmetria of thought and the universal cerebellar transform theories. Cortex 100:140–148.

Guell X, Gabrieli JDE, Schmahmann JD. 2018b. Triple representation of language, working memory, social and emotion processing in the cerebellum: convergent evidence from task and seed-based resting-state fMRI analyses in a single large cohort. Neuroimage 172:437–449.

Guell X, D'Mello M, Hubbard N, Romeo R, Gabrieli JDE, Whitfield-Gabrieli S, et al. 2019a. Functional territories of human dentate nucleus. Cereb Cortex [Epub ahead of print]; DOI: 10.1101/608620.

Guell X, Goncalves M, Kaczmarzyk JR, Gabrieli JDE, Schmahmann JD, Ghosh SS. 2019b. LittleBrain: a gradient-based tool for the topographical interpretation of cerebellar neuroimaging findings. PLoS One 14:e0210028.

Guell X, Schmahmann JD, Gabrieli J, Ghosh SS. 2018c. Functional gradients of the cerebellum. eLife 7:pii:e36652.

Habas C. 2010. Functional imaging of the deep cerebellar nuclei: a review. Cerebellum 9:22–28.

Hanaie R, Mohri I, Kagitani-Shimono K, Tachibana M, Azuma J, Matsuzaki J, et al. 2013. Altered microstructural connectivity of the superior cerebellar peduncle is related to motor dysfunction in children with autistic spectrum disorders. Cerebellum 12:645–656.

Hanaie R, Mohri I, Kagitani-Shimono K, Tachibana M, Matsuzaki J, Hirata I, et al. 2018. Aberrant cerebellar-cerebral functional connectivity in children and adolescents with autism spectrum disorder. Front Hum Neurosci 12:454.

He N, Langley J, Huddleston DE, Ling H, Xu H, Liu C, et al. 2017. Improved neuroimaging atlas of the dentate nucleus. Cerebellum 16:951–956.

Hoshi E, Tremblay L, Feger J, Carras PL, Strick PL. 2005. The cerebellum communicates with the basal ganglia. Nat Neurosci 8:1491–1493.

Igelstrom KM, Webb TW, Graziano MSA. 2017. Functional connectivity between the temporoparietal cortex and cerebellum in autism spectrum disorder. Cereb Cortex 27:2617–2627.

Ito M. 1993. Movement and thought: identical control mechanisms by the cerebellum. Trends Neurosci 16:448–450; discussion 453–454.

Jack A, Pelphrey KA. 2015. Neural correlates of animacy attribution include neocerebellum in healthy adults. Cereb Cortex 25:4240–4247.

Jeong JW, Chugani DC, Behen ME, Tiwari VN, Chugani HT. 2012. Altered white matter structure of the dentatorubrothalamic pathway in children with autistic spectrum disorders. Cerebellum 11:957–971.

Joshi G, Arnold Anteraper S, Patil KR, Semwal M, Goldin RL, Furtak SL, et al. 2017. Integration and segregation of default mode network resting-state functional connectivity in transition-age males with high-functioning autism spectrum disorder: a proof-of-concept study. Brain Connect 7:558–573.

Kelly RM, Strick PL. 2003. Cerebellar loops with motor cortex and prefrontal cortex of a nonhuman primate. J Neurosci 23:8432–8444.

Kennedy DP, Courchesne E. 2008. Functional abnormalities of the default network during self- and other-reflection in autism. Soc Cogn Affect Neurosci 3:177–190.

Khan AJ, Nair A, Keown CL, Datko MC, Lincoln AJ, Muller RA. 2015. Cerebro-cerebellar resting-state functional connectivity in children and adolescents with autism spectrum disorder. Biol Psychiatry 78:625–634.

Kuper M, Dimitrova A, Thurling M, Maderwald S, Roths J, Elles HG, et al. 2011. Evidence for a motor and a non-motor domain in the human dentate nucleus—an fMRI study. Neuroimage 54:2612–2622.

Lord C, Risi S, Lambrecht L, Cook EH Jr, Leventhal BL, DiLavore PC, et al. 2000. The autism diagnostic observation schedule-generic: a standard measure of social and communication deficits associated with the spectrum of autism. J Autism Dev Disord 30:205–223.

Middleton FA, Strick PL. 1994. Anatomical evidence for cerebellar and basal ganglia involvement in higher cognitive function. Science 266:458–461.

Noonan SK, Haist F, Muller RA. 2009. Aberrant functional connectivity in autism: evidence from low-frequency BOLD signal fluctuations. Brain Res 1262:48–63.

Olivito G, Clausi S, Laghi F, Tedesco AM, Baiocco R, Mastropasqua C, et al. 2017. Resting-state functional connectivity changes between dentate nucleus and cortical social brain regions in autism spectrum disorders. Cerebellum 16:283–292.

Olivito G, Lupo M, Laghi F, Clausi S, Baiocco R, Cercignani M, et al. 2018. Lobular patterns of cerebellar resting-state connectivity in adults with autism spectrum disorder. Eur J Neurosci 47:729–735.

Padmanabhan A, Lynch CJ, Schaer M, Menon V. 2017. The default mode network in autism. Biol Psychiatry Cogn Neurosci Neuroimaging 2:476–486.

Pelphrey K. 2017. Charting a course for autism biomarkers. Biol Psychiatry 82:155–156.

Ramnani N. 2014. Automatic and controlled processing in the corticocerebellar system. Prog Brain Res 210:255–285.

Raymond JL, Medina JF. 2018. computational principles of supervised learning in the cerebellum. Annu Rev Neurosci 41:233–253.

Reed CL, Caselli RJ. 1994. The nature of tactile agnosia: a case study. Neuropsychologia 32:527–539.

Riva F, Triscoli C, Lamm C, Carnaghi A, Silani G. 2016. Emotional egocentricity bias across the life-span. Front Aging Neurosci 8:74.

Rojas DC, Peterson E, Winterrowd E, Reite ML, Rogers SJ, Tregellas JR. 2006. Regional gray matter volumetric changes in autism associated with social and repetitive behavior symptoms. BMC Psychiatry 6:56.

Salmi J, Roine U, Glerean E, Lahnakoski J, Nieminen-von Wendt T, Tani P, et al. 2013. The brains of high functioning autistic individuals do not synchronize with those of others. Neuroimage Clin 3:489–497.

Sathyanesan A, Zhou J, Scafidi J, Heck DH, Sillitoe RV, Gallo V. 2019. Emerging connections between cerebellar development, behaviour and complex brain disorders. Nat Rev Neurosci 20:298–313.

Saxe R, Wexler A. 2005. Making sense of another mind: the role of the right temporo-parietal junction. Neuropsychologia 43:1391–1399.

Schmahmann JD. 1991. An emerging concept. The cerebellar contribution to higher function. Arch Neurol 48:1178–1187.

Schmahmann JD. 1996. From movement to thought: anatomic substrates of the cerebellar contribution to cognitive processing. Hum Brain Mapp 4:174–198.

Schmahmann JD, Sherman JC. 1998. The cerebellar cognitive affective syndrome. Brain 121 (Pt 4):561–579.

Shukla DK, Keehn B, Lincoln AJ, Muller RA. 2010. White matter compromise of callosal and subcortical fiber tracts in children with autism spectrum disorder: a diffusion tensor imaging study. J Am Acad Child Adolesc Psychiatry 49:1269–1278, 1278.e1–1278.e2.

Skefos J, Cummings C, Enzer K, Holiday J, Weed K, Levy E, et al. 2014. Regional alterations in purkinje cell density in patients with autism. PLoS One 9:e81255.

Silani G, Bird G, Brindley R, Singer T, Frith C, Frith U. 2008. Levels of emotional awareness and autism: an fMRI study. Soc Neurosci 3:97–112.

Smith REW, Avery JA, Wallace GL, Kenworthy L, Gotts SJ, Martin A. 2019. Sex differences in resting-state functional connectivity of the cerebellum in autism spectrum disorder. Front Hum Neurosci 13:104.

Soghomonian JJ, Zhang K, Reprakash S, Blatt GJ. 2017. Decreased parvalbumin mRNA levels in cerebellar Purkinje cells in autism. Autism Res 10:1787–1796.

Steele CJ, Anwander A, Bazin PL, Trampel R, Schaefer A, Turner R, et al. 2017. Human cerebellar sub-millimeter diffusion imaging reveals the motor and non-motor topography of the dentate nucleus. Cereb Cortex 27:4537–4548.

Stoodley CJ, D'Mello AM, Ellegood J, Jakkamsetti V, Liu P, Nebel MB, et al. 2017. Altered cerebellar connectivity in autism and cerebellar-mediated rescue of autism-related behaviors in mice. Nat Neurosci 20:1744–1751.

Stoodley CJ, Schmahmann JD. 2009. Functional topography in the human cerebellum: a meta-analysis of neuroimaging studies. Neuroimage 44:489–501.

Stoodley CJ, Valera EM, Schmahmann JD. 2012. Functional topography of the cerebellum for motor and cognitive tasks: an fMRI study. Neuroimage 59:1560–1570.

Sultan F, Hamodeh S, Baizer JS. 2010. The human dentate nucleus: a complex shape untangled. Neuroscience 167:965–968.

Verly M, Verhoeven J, Zink I, Mantini D, Peeters R, Deprez S, et al. 2014. Altered functional connectivity of the language network in ASD: role of classical language areas and cerebellum. Neuroimage Clin 4:374–382.

Whitfield-Gabrieli S, Nieto-Castanon A. 2012. Conn: a functional connectivity toolbox for correlated and anticorrelated brain networks. Brain Connect 2:125–141.

Yerys BE, Gordon EM, Abrams DN, Satterthwaite TD, Weinblatt R, Jankowski KF, et al. 2015. Default mode network segregation and social deficits in autism spectrum disorder: evidence from non-medicated children. Neuroimage Clin 9: 223–232.

Yip J, Soghomonian JJ, Blatt GJ. 2007. Decreased GAD67 mRNA levels in cerebellar Purkinje cells in autism: pathophysiological implications. Acta Neuropathol 113:559–568.

Address correspondence to:
Sheeba Arnold Anteraper
Department of Psychology
Northeastern University
805 Columbus Ave.
ISEC 672C
Boston, MA 02120

E-mail: s.anteraper@northeastern.edu